Available online at www.sciencedirect.com
ScienceDirect
Journal of Nuclear Materials 367–370 (2007) 411–416
journal of nuclear materials
www.elsevier.com/locate/jnucmat

Effect of a high helium content on the flow and fracture properties of a 9Cr martensitic steel

J. Henry [a,*], L. Vincent [a], X. Averty [b], B. Marini [a], P. Jung [c]

[a] CEA Saclay, DEN/DMN/SRMA, F-91191 Gif-sur-Yvette cedex, France
[b] CEA Saclay, SEMI, F-91191 Gif-sur-Yvette cedex, France
[c] Institut für Festkörperforschung, Forschungszentrum Jülich, D-52425 Jülich, Germany

Abstract

An experimental characterization was conducted of helium effects on the mechanical properties of a 9Cr martensitic steel. Six sub-size Charpy samples were implanted in the notch region at 250 °C with 0.25 at.% helium and subsequently tested in 3-point bending at room temperature. Brittle fracture mode (cleavage and intergranular fracture) was systematically observed in the implanted zones of the samples. Finite element calculations of the tests, using as input the tensile properties measured on a helium loaded sample, were performed in order to determine the fracture stress at the onset of brittle crack propagation. Preliminary TEM investigations of the implantation-induced microstructure revealed a high density of small helium bubbles.

1. Introduction

Ferritic/martensitic steels are prime candidate materials for future fusion plants or spallation devices due to their excellent thermomechanical properties and radiation resistance above about 400 °C in a fission spectrum. However, the possible detrimental effect of helium generated by transmutation on the mechanical properties of these steels is of special concern. Although a considerable amount of experimental work has been devoted to this issue in the past, using in particular the implantation or the Ni, B, or Fe doping techniques, the extent to which helium modifies the tensile and fracture properties of these steels is still a matter of debate. It was recently shown [1] that a large concentration of helium (0.5 at.%) can drastically degrade the tensile properties of 9Cr martensitic steels, leading to a complete loss of ductility and a fully intergranular fracture mode. In the present study, we have investigated the effects of a lower helium content (0.25 at.%, equivalent to 25 MW-y/m^2 service at the near-plasma zone of a fusion blanket) on the tensile and fracture properties of a 9Cr martensitic steel. To this end, sub-size Charpy specimens were helium implanted and subsequently submitted to three point bending tests. The results were analyzed based on finite element calculations using as input the tensile properties measured following helium implantation of miniature specimens.

* Corresponding author. Tel.: +33 1 69088508; fax: +33 1 69087130.
E-mail address: jean.henry@cea.fr (J. Henry).

0022-3115/$ - see front matter © 2007 Elsevier B.V. All rights reserved.
doi:10.1016/j.jnucmat.2007.03.122

A preliminary transmission electron microscopy (TEM) investigation of the implantation-induced microstructure is also presented.

2. Experimental

2.1. Materials, specimens and He implantation

Miniature tensile specimens, 100 μm in thickness, 28 mm total length, with a gauge length of 12 mm and 2 mm width were cut by spark-erosion from a sheet of a mod 9Cr–1Mo alloy, with a composition of 0.105% C, 8.26% Cr, 0.95% Mo, 0.2% V, 0.075% Nb, 0.13% Ni, 0.38% Mn, 0.0055 N, 0.009 P, 0.43% Si, Bal Fe, in wt%. The specimens were subsequently heat treated to obtain a tempered martensitic microstructure. Sub-size Charpy specimens (KLST geometry, $27 \times 4 \times 3\ mm^3$) were prepared from a normalized-and-tempered 15 mm thick plate of a second mod 9Cr–1Mo heat, due to insufficient remaining material from the first heat. The composition of this second heat was 0.1% C, 8.73% Cr, 0.99% Mo, 0.19% V, 0.23% Ni, 0.43% Mn, 0.029% N, 0.021% P, 0.32% Si, Bal Fe. More details about heat treatments, specimens geometry and preparation can be found in [2,3].

Tensile specimens were implanted using a 23 MeV ^{4}He beam delivered by the Jülich cyclotron, which was degraded by a rotating wheel with 24 Al foils of different thicknesses, in order to achieve a homogeneous implantation throughout the thickness of the specimens. The implanted concentration was close to 0.25 at.%, which corresponds to approximately 0.4 dpa of displacement damage, as calculated by the SRIM code, using a displacement threshold energy of 40 eV. The implantation rate was about 0.015 appm He/s. The specimens were heated by the beam current, while the temperature was adjusted to 250 °C by flowing helium gas. The specimens temperature was monitored by infrared pyrometry. Additional details regarding the implantation conditions can be found in [1].

Sub-size Charpy specimens were implanted with a degraded 34 MeV ^{3}He beam. They were homogeneously loaded with 0.25 at.% He up to the total range of the ^{3}He particles, i.e. 240 μm. As with the tensile specimens, the Charpy specimens were heated by the beam current, with temperature adjustment by the flowrate of the coolant. There was a significant temperature gradient between the notched side of the specimen, facing the beam, and the back side, where pyrometry measurements were taken. The temperature of the implanted zone was determined by finite element calculations and held at 250 °C, as described in [3] in which the implantation conditions are further detailed. The average implantation rate for the Charpy specimens was about 0.01 appm/s.

2.2. Tensile and bending tests

Tensile testing was carried out in a tensile device for miniature specimens at a strain rate of about 10^{-4}/s. Strains were calculated from length change divided by the effective gauge length.

The three point bending tests on helium implanted sub-size Charpy specimens were performed in crosshead displacement control using a crosshead speed of 0.1 mm/min. The testing machine was equipped with a high frequency data acquisition system in order to allow the detection of possible 'pop-in' phenomena inside the implanted zone below the notch.

2.3. Transmission electron microscopy (TEM) observations

A disc 2 mm in diameter was punched from the gauge section of a tensile specimen implanted at 250 °C and tested at room temperature. This disc was subsequently electropolished and microstructural characterization was carried out using a JEOL 2010F microscope operated at 200 kV. For number densities measurements, the local specimen thickness was evaluated by electron energy loss spectroscopy, using 120 nm as the value for the mean free path of inelastic scattering processes.

3. Results

3.1. Tensile tests

Fig. 1 shows strain–stress curves for unimplanted and implanted mod 9Cr–1Mo steel tested at room temperature. Strong hardening and loss of ductility occurred as a result of helium implantation. The fracture mode was predominantly ductile, as shown by the scanning electron microscopy (SEM) micrographs (Fig. 2). Nevertheless, in addition to the ductile dimple fracture appearance, numerous secondary cracks are present, some of which seem to follow grain boundaries.

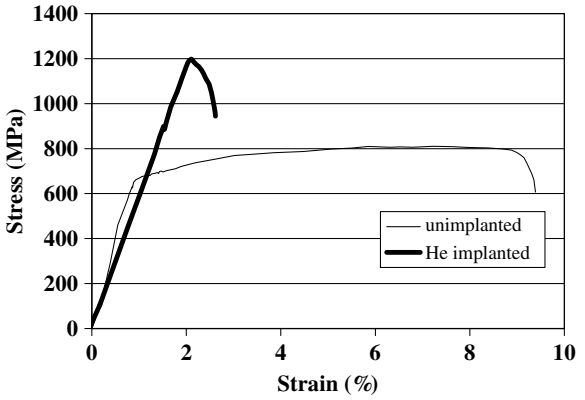

Fig. 1. Tensile curves (engineering stress and strain) of mod 9Cr–1Mo steel unimplanted and implanted at 250 °C with 0.25 at.% He. The tests were carried out at room temperature.

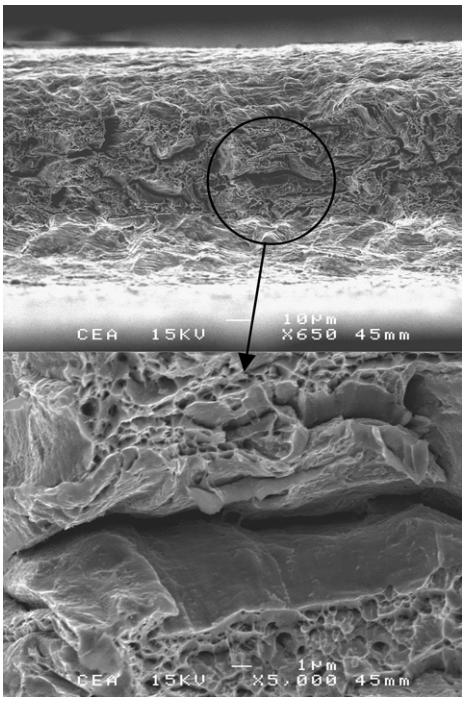

Fig. 2. SEM micrographs showing the fracture surface of a 9Cr–1Mo tensile specimen implanted to 0.25 at.% He at 250 °C and tested at room temperature.

3.2. Bending tests

Static bending tests were carried out at room temperature on six miniature Charpy specimens implanted at 250 °C in the notch region with 0.25 at.% helium. Fig. 3 presents the bending curves, which all display the same feature, a so-called 'pop-in', in a narrow applied load range. Such a feature corresponds to brittle crack initiation and propagation in the implanted zone, followed by crack arrest in the unimplanted area of the sample. SEM observations of tested samples have confirmed this analysis. Two distinct zones can be seen on the fracture surfaces as shown in Fig. 4. Just below the notch root, the first zone has a fully brittle appearance, with both intergranular and cleavage fracture modes. The depth of this first zone is exactly equal to the range of the ^{3}He particles, i.e. 240 µm, which indicates that it corresponds to the implanted region of the sample. The second zone, which does not contain helium, has a fully ductile appearance, as expected for mod 9Cr–1Mo steel in a static bending test at room temperature.

3D finite element calculations of the bending tests were carried out in order to obtain the local strain and stress fields. These calculations were performed using two constitutive behaviours: one for unimplanted mod 9Cr–1Mo steel, the other for the steel charged with helium, which was derived from the tensile curve shown in Fig. 1. The values of the maximum principal stress σ_1 as a function of distance to the notch root were calculated and are given in Fig. 5. Curves corresponding to calculations performed for the case of unimplanted mod 9Cr–1Mo submitted to bending tests at −170 °C [3], i.e. in the brittle domain where the fracture mode is 100% cleavage, were added as well. In each case, two curves are plotted: they represent the σ_1 evolution for an opening displacement equal to the highest, respectively lowest, value at failure (or at the onset of the 'pop-in') measured experimentally.

Fig. 5 shows that significantly higher σ_1 values were reached in the unimplanted samples tested in the brittle domain compared to the case of helium implanted samples tested at room temperature. These high stress values extend over a large distance from the notch root, whereas in implanted samples, σ_1 quickly drops with increasing distance from the notch.

3.3. Microstructure

A preliminary investigation of the microstructure induced by the implantation of 0.25 at.% helium at 250 °C was performed by TEM. The implantation-induced defect structure consists of small defect clusters ('black dots') and dislocation loops. Moreover, under phase contrast conditions, a high density of small helium bubbles was detected as shown in Fig. 6. Their number density was evaluated to be

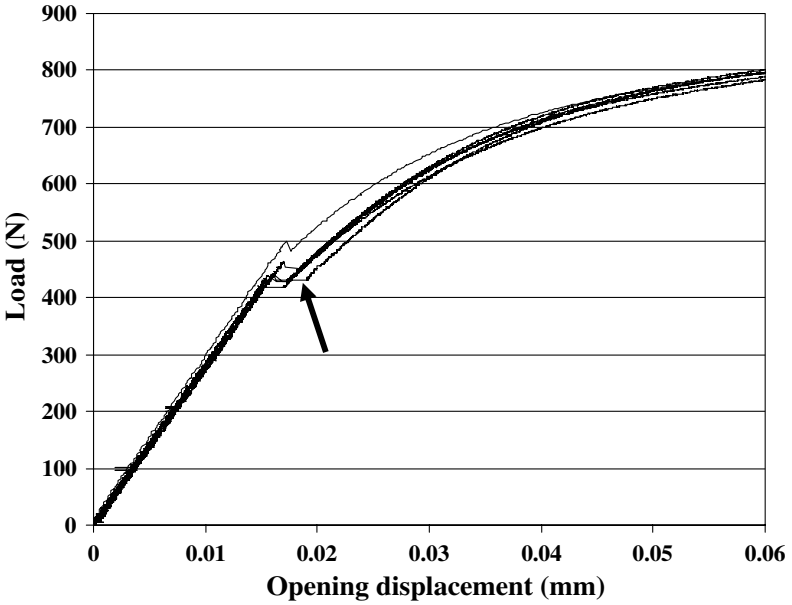

Fig. 3. Load versus opening displacement curves for mod 9Cr–1Mo implanted at 250 °C with 0.25 at.% He and tested in three point bending at room temperature. For all specimens, a 'pop-in' (indicated by the arrow) occurred during testing.

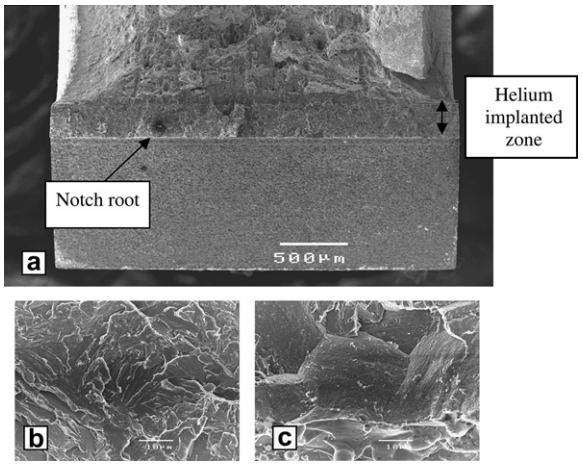

Fig. 4. SEM micrographs showing the fracture surface of a mod 9Cr–1Mo sub-size Charpy specimen implanted with 0.25 at.% helium and tested in three point bending at room temperature: (a) partial view of the broken specimen; (b) and (c) details of the fracture surface in the brittle, helium implanted zone.

about $3–4 \times 10^{23}$ m^{-3}. No precise bubble size determination was carried out; however, the average detectable bubble radius appears to be less then 1 nm.

4. Discussion

The TEM analysis has shown that in addition to black dots/dislocation loops, the implantation microstructure consists of a high density of nanometer sized bubbles while the tensile tests have revealed a large increase in yield strength. There is today no consensus regarding the effects of small helium bubbles on the yield strength of irradiated alloys; however, there is increasing evidence that they can contribute significantly to hardening. For instance, Hunn et al. [4] have shown by irradiating 316L austenitic steel at 200 °C with either Fe or He ions, that above a threshold helium concentration, the hardening induced by the helium implantation was well above that measured for the Fe irradiation, for the same displacement damage. This was interpreted as due to the presence of a high number density of helium bubbles. In a previous study [2], the very large amount of hardening observed following implantation at 250 °C to 0.5 at.% He of 9Cr–1Mo and mod 9Cr–1Mo steels was mainly attributed to the high density (above 8×10^{23} m^{-3}) of tiny helium bubbles detected by SANS experiments. This conclusion was based on a comparison of yield stress increases following either irradiation in a fission spectrum or helium implantation. Also, Dai et al. [5] have performed tensile tests on mod 9Cr–1Mo samples irradiated in a spallation spectrum at temperatures below 300 °C. They interpreted the measured dose dependence of the increases in yield strength as evidence for a significant contribution of gas bubbles. TEM work performed on samples

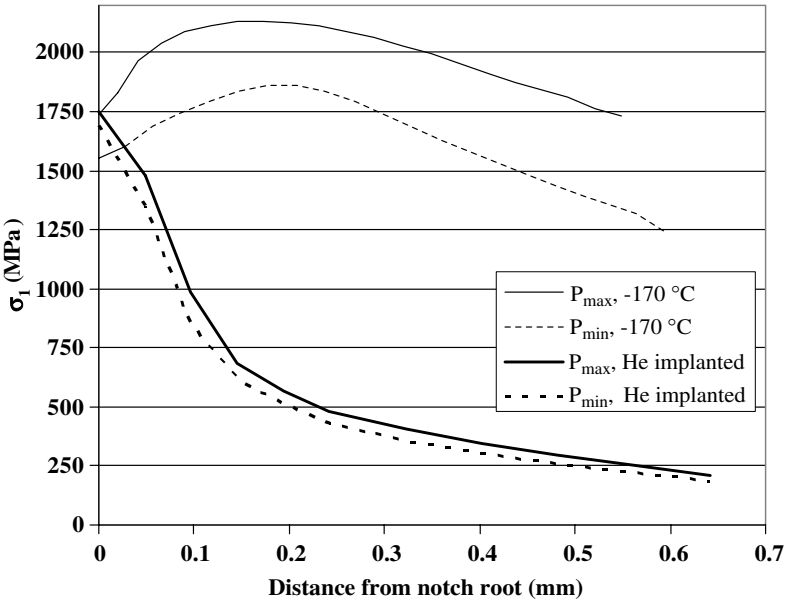

Fig. 5. Evolution of the maximum principal stress σ_1 as a function of the distance to the notch root. In the labels, P_{max} (resp. P_{min}) indicate the curves which correspond to the highest (resp. lowest) opening displacement at the onset of 'pop-in' crack propagation. Curves corresponding to unimplanted samples tested in three point bending at −170 °C [3] are added as well for comparison (in which case the calculations were performed for the highest/lowest measured displacements at failure).

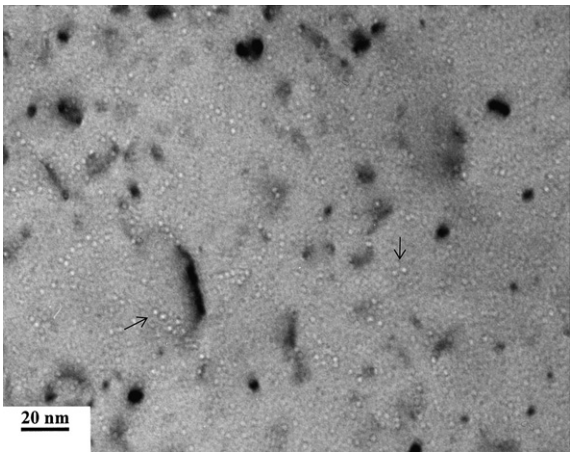

Fig. 6. TEM micrograph showing the bubble microstructure in mod 9Cr–1Mo steel implanted to 0.25 at.% He at 250 °C. Underfocus imaging conditions ($\delta f = -2000$ nm). Two typical bubles are indicated by the arrows.

irradiated in similar conditions as the tensile specimens revealed nanometric bubbles with densities slightly above 5×10^{23} m^{-3}.

In addition, Osetsky et al. [6] have modelled at the atomic scale the interaction of an edge dislocation with voids in iron. They showed that voids are strong obstacles even for diameters down to 1 nm. It should be mentioned, however, that Wirth et al. [7] concluded, based on MD simulations in Al, that voids are rather weak barriers, while helium filled cavities offer only slightly more resistance to dislocation motion. Clearly additional work, both modelling and experiments, is needed to better evaluate the contribution of helium bubbles to hardening.

However, helium has more of an effect on the mechanical properties of martensitic steels than just its potential role in hardening. Odette et al. [8] have recently analyzed the published paired data sets on irradiation-induced increases in yield stress, $\Delta\sigma$, and DBTT shifts, ΔT. Their conclusion is that above a concentration of several hundred appm helium, the increase of the $c = \Delta\sigma/\Delta T$ ratio indicates that non-hardening helium embrittlement is probably occuring. The drastic embrittlement displayed in this work by the specimens tested in three point bending is clearly a manifestation of such a phenomenon. It is clearly more than only the result of the hardening due to implantation. Indeed, helium induces a reduction in the critical stress for brittle fracture, since, for the same sample geometry, brittle fracture occurred in the implanted zones for values of the maximum principal stress below 1750 MPa, whereas at failure, the highest values of σ_1 were in the range

1850–2150 MPa for the unimplanted samples tested at −170 °C. Obviously, the implanted helium lowers the grain boundary cohesion as a significant amount of intergranular areas were observed on the fracture surfaces of the samples containing helium, while the fracture appearance was almost fully cleavage in the unimplanted case [3]. The fact that the helium implanted tensile sample broke in a predominantly ductile manner, although some intergranular separation was detected, is probably due to the low stress triaxiality in a tensile test performed on a very thin specimen. By contrast, the triaxiality ratio is higher in the case of bending tests on notched specimens, which promotes brittle fracture modes.

The mechanical analysis of the bending tests, as illustrated in Fig. 5, shows that following implantation of 0.25 at.% helium at 250 °C, mod 9Cr–1Mo is more brittle at room temperature than the unimplanted steel tested at −170 °C. Indeed, the fracture toughness was tentatively evaluated in both cases using the Beremin model of brittle fracture [3]. The predicted mean toughness at room temperature for the implanted material was evaluated to be about 17 MPa $m^{1/2}$, compared to 35 MPa $m^{1/2}$ for the unimplanted steel at −170 °C.

5. Summary/conclusion

Miniature tensile and sub-size Charpy specimens have been implanted at 250 °C with 0.25 at.% helium and subsequently submitted to mechanical tests at room temperature. While tensile testing revealed strong hardening and a predominantly ductile fracture mode, a fully brittle fracture mode, with both cleavage and intergranular fracture, was systematically observed in the implanted areas of the Charpy specimens tested in static three point bending. Preliminary TEM investigations showed that in addition to implantation-induced damage (black dots and dislocation loops), the implanted sample contained a high density of nanometric bubbles which may contribute significantly to hardening. Furthermore, the finite element analysis of the bending tests, together with the fractographic examinations, demonstrated that the implanted helium has induced a decrease in the critical stress for intergranular fracture. Additional bending tests combined with TEM microstructural studies will be carried out on specimens implanted to lower helium contents and/or different temperatures to advance the characterization and understanding of helium effects on the fracture properties of 9Cr martensitic steels.

References

[1] P. Jung, J. Henry, J. Chen, J.-C. Brachet, J. Nucl. Mater. 318 (2003) 241.
[2] J. Henry, M.-H. Mathon, P. Jung, J. Nucl. Mater. 318 (2003) 249.
[3] J. Henry, L. Vincent, X. Averty, B. Marini, P. Jung, J. Nucl. Mater. 356 (2006) 78.
[4] J. Hunn, E. Lee, T. Byun, L. Mansur, J. Nucl. Mater. 282 (2000) 131.
[5] Y. Dai, X. Jia, K. Farrell, J. Nucl. Mater. 318 (2003) 192.
[6] Y. Osetsky, D. Bacon, V. Mohles, Phil. Mag. 83 (2003) 3623.
[7] B. Wirth, G. Odette, J. Marian, L. Ventelon, J. Young-Vandersall, L. Zepeda-Ruiz, J. Nucl. Mater. 329–333 (2004) 103.
[8] G.R. Odette, T. Yamamoto, H. Kishimoto, Fusion Materials Semiannual Progress Report for the Period Ending, December 31, 2003, DOE-ER-0313/35, p. 80.